The Biliverdin Chromophore Binds Covalently to a Conserved Cysteine Residue in the N-Terminus of *Agrobacterium* Phytochrome Agp1[†]

Tilman Lamparter,*[,‡] Montserrat Carrascal,[§] Norbert Michael,[‡] Enriqueta Martinez,[‡] Gregor Rottwinkel,[‡] and Joaquin Abian[§]

Freie Universität Berlin, Pflanzenphysiologie, Königin Luise Strasse 12-16, D-14195 Berlin, Germany, and Structural and Biological Mass Spectrometry Unit, IIBB-CSIC, IDIBAPS, Rosellon 161, 7 Planta E, 08036 Barcelona, Spain

Received September 19, 2003; Revised Manuscript Received January 28, 2004

ABSTRACT: Phytochromes are widely distributed biliprotein photoreceptors. Typically, the chromophore becomes covalently linked to the protein during an autocatalytic lyase reaction. Plant and cyanobacterial phytochromes incorporate bilins with a ring A ethylidene side chain, whereas other bacterial phytochromes utilize biliverdin as chromophore, which has a vinyl ring A side chain. For *Agrobacterium* phytochrome Agp1, site-directed mutagenesis provided evidence that biliverdin is bound to cysteine 20. This cysteine is highly conserved within bacterial homologues, but its role as attachment site has as yet not been proven. We therefore performed mass spectrometry studies on proteolytic holopeptide fragments. For that purpose, an Agp1 expression vector was re-engineered to produce a protein with an N-terminal affinity tag. Following proteolysis, the chromophore co-purified with a ca. 5 kDa fragment during affinity chromatography, showing that the attachment site is located close to the N-terminus. Mass spectrometry analyses performed with the purified chromopeptide confirmed the role of the cysteine 20 as biliverdin attachment site. We also analyzed the role of the highly conserved histidine 250 by site-directed mutagenesis. The homologous amino acid plays an important but yet undefined role in plant phytochromes and has been proposed as chromophore attachment site of *Deinococcus* phytochrome. We found that in Agp1, this amino acid is dispensable for covalent attachment, but required for tight chromophore−protein interaction.

Phytochromes are photochromic photoreceptors that were found in plants, bacteria, fungi, and slime moulds (*1*−*3*). Typical phytochrome proteins consist of an N-terminal sensory module, which contains all features for chromophore incorporation and spectral activity, and a C-terminal signaling module, which is a histidine kinase in many bacterial phytochromes (see Figure 1 for domain structure of *Agrobacterium* phytochrome Agp1). The chromophore, an open chain tetrapyrrole (bilin), varies between species. Seed plant phytochromes have phytochromobilin as natural chromophore (*4*), whereas phytochromes of the green alga *Mesotaenium* (*5*) and the cyanobacterium *Synechocystis* PCC 6803 (*6*) carry phycocyanobilin (PCB[1]) as natural chromophore. Both bilins have a ring A ethylidene side chain, which forms a covalent link with a conserved cysteine residue during chromophore assembly (*4*). Recombinant plant and cyanobacterial phytochromes assemble with both bilins in vitro (*7*−*9*). Recently, phytochromes from proteobacteria and *Deinococcus* have been described that incorporate biliverdin (BV), the proposed natural chromophore of these species (*1*, *10*−*12*). Biliverdin differs from the other chromophores because it has a ring A vinyl side chain. In phytochrome Agp1 of *Agrobacterium tumefaciens*, this side chain is required for covalent attachment (*13*).

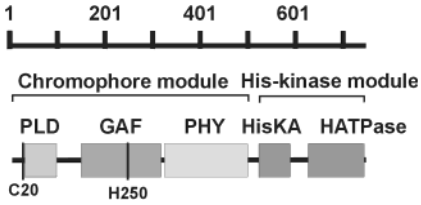

FIGURE 1: Domain arrangement of *Agrobacterium* phytochrome Agp1. PLD: PAS-like domain. The positions of the chromophore-binding Cys[20] and the mutated His[250] are indicated.

The chromophore-binding cysteine residue of plant phytochromes lies in the so-called GAF domain of the protein (*14*). This residue is conserved in all plant phytochromes and in some cyanobacterial orthologs such as Cph1 (*15*) or CphA (*9*). Other cyanobacterial phytochromes and orthologs from all other bacteria and fungi do not contain a cysteine residue at the homologous position (*9*−*12*). The appearance of this cysteine residue in cyanobacteria correlates with the possibility of these cells to reduce BV to PCB.

Although the homologous cysteine is lacking in BV-binding phytochromes, this chromophore is also covalently attached to the protein (*1*, *11*). The site for covalent attachment was initially analyzed for phytochrome from *Deinococcus radiodurans*. These studies were performed

[†] The work was supported by Deutsche Forschungsgemeinschaft, Sfb 498, TP B2.

* Corresponding author. Tel.: +49 (0)30 838 54918. Fax: +49-(0)30 838 84357. E-mail: lamparte@zedat.fu-berlin.de.

[‡] Freie Universität Berlin.

[§] IDIBAPS.

[1] Abbreviations: BV, biliverdin; DTBN, 5,5′-dithiobis(2-nitrobenzoic acid); MALDI-TOFMS, matrix-assisted laser desorption−ionization time-of-flight mass spectrometry; nESI-ITMS, nanoelectrospray ion trap mass spectrometry; MS/MS, tandem mass spectrometry; PAGE polyacrylamide gel electrophoresis; PCB, phycocyanobilin; V8, endoproteinase Glu-C.

10.1021/bi035693l CCC: $27.50
Published on Web 03/02/2004

with PCB, since the role of BV as natural chromophore was unknown. Site-directed mutagenesis and mass spectrometry analyses provided evidence that PCB is covalently bound to a histidine residue which is highly conserved in phytochromes (*10*). In plant orthologs, this histidine residue is located immediately C-terminal of the chromophore-binding cysteine. Other BV-binding phytochromes, CphB from *Calothrix* (*9*) and Agp1 from *Agrobacterium tumefaciens* (*11*), also form photoactive adducts with PCB, but in these phytochromes, PCB is bound in a noncovalent manner to the protein.

In the case of *Agrobacterium* Agp1, blocking experiments suggested that BV is covalently attached to a cysteine residue. Site-directed mutagenesis revealed a cysteine close to the N-terminus of the protein as putative chromophore attachment site (*11*). This residue is conserved in the group of BV-binding phytochromes and might therefore be used as general attachment site of BV phytochromes. However, mutagenesis experiments provide only indirect evidence for the role of the cysteine residue. We therefore performed mass spectrometry analyses on proteolytic holopeptide fragments to confirm the role of the cysteine residue. To allow for convenient purification of a holopeptide proteolysis fragment, the protein was re-engineered in such a way that this peptide should bind to a Ni^{2+}-affinity matrix via an N-terminal polyhistidine tag. We obtained a ~5 kDa fragment which was analyzed by matrix assisted laser desorption time-of-flight mass spectrometry (MALDI-TOFMS) and nanoelectrospray tandem mass spectrometry on an ion trap instrument (nESI-IT MS/MS). Further experiments were performed to study the role of the highly conserved histidine residue.

EXPERIMENTAL PROCEDURES

Cloning of the Expression Construct for Agp1-M13 and H250A. Molecular cloning of expression vectors from the template plasmid pAG1 (*11*) were performed by inverted PCR using error checking PfuTurbo DNA Polymerase (Stratagene, La Jolla, CA), followed by DpnI digestion of the template, agarose gel purification, phosphorylation, and blunt end ligation with T4-Kinase and T4 Ligase (NEB, Beverly, MA) and transformation into *E. coli* Xl1blue cells. In the first step, the region coding for the C-terminal histidine tag was removed to obtain plasmid pAG-M0 using the primers TAATTAGCTGAGCTTGGACTCCTGTTG and GGCAATTTTTTCCTCTTCAACTTTCGTAAC. In the next step, the region coding for amino acids 1−10 of pAG-M0 was removed and replaced by a sequence coding for MHHHHHH, using the primers CATCACCATCACCATCACAGTTCACATACGCCGAAACTGGATAGTTGC and CATGGTTAATTTCTCCTCTTTAATGAATTCTG. The resulting plasmid is termed pAG1-M13, the encoded protein Agp1-M13. Positive clones after each round of sub-cloning were selected by protein expression assays. Correct cloning was confirmed by DNA-sequencing.

The expression clone for the H250A mutant was generated from pAG1 using the QuikChange site-directed mutagenesis kit (Stratagene).

Protein Expression and Purification. Details of protein expression and purification are given in earlier publications (*11*, *16*). Expression clones were grown in 1 L cultures (rich broth medium with ampicillin) at 30 °C until the cell density reached an OD_{600} of 0.5; thereafter, protein expression was induced by addition of 50 μM IPTG to the growth medium. After 16 h incubation at 20 °C, the cell density reached levels of OD_{600} between 1.5 and 1.8. The cells were resuspended in 10 mL extraction buffer (300 mM NaCl, 50 mM Tris/Cl, 5 mM EDTA, and 10 mM DTT, pH 7.8) and extracted with a French Pressure Cell. After centrifugation, proteins of the supernatant were precipitated with ammonium sulfate, resolved in EDTA-free buffer (300 mM NaCl, 50 mM Tris/HCl, 10 mM imidazole, pH 7.8), centrifuged again, and subjected to Ni^{2+}-affinity chromatography. Agp1 was eluted with imidazole (300 mM NaCl, 50 mM Tris/HCl, 250 mM imidazole, pH 7.8) and subjected to ammonium sulfate precipitation. The protein was finally resuspended in 300 mM NaCl, 50 mM Tris/HCl, 5 mM EDTA, pH 7.8 at a concentration of 13 mg/mL and cleared by centrifugation. To obtain holo-Agp1, BV (Frontier Scientific, Carnforth, U.K.) was added at ca. 1.5-fold molar excess to the apoprotein solution. Free BV was removed by size exclusion chromatography on a 2.5 × 100 cm Sephacryl S-300 (Amersham Bioscience) column (*11*).

Chromophore−protein interaction was analyzed by size separation on NAP columns (Amersham Biotec, Freiburg, Germany) and UV−vis spectroscopy as described before (*13*). This assay was performed both in the native state (without SDS) or after SDS-dissociation of noncovalent associations. The percentage of bound chromophore was calculated by comparing the ratio between chromophore absorbance (usually around 700 nm) and protein absorbance (280 nm) after and before column separation.

Proteolysis and PAGE. For standard Endoproteinase-Glu-C (V8) proteolysis, 0.5 mL of holo- or apo-Agp1-M13 solution was precipitated with ammonium sulfate (final concentration 1.65 M) and the pelleted protein resuspended in Tris buffer (50 mM Tris/HCl, pH 7.8) containing 0.5% SDS and 100 units V8 protease. The sample was incubated for 20 h at 20 °C. The N-terminal fragment was purified by Ni^{2+}-affinity chromatography using 5 mL Ni^{2+}-NTA-agarose (Qiagen, Hilden, Germany) columns. The columns were equilibrated with Tris buffer, the sample was diluted with the same buffer to reduce the SDS concentration to 0.1% and loaded to the column. After washing the column with 20 mL Tris buffer, bound peptides were eluted with 250 mM imidazole, 50 mM Tris/HCl, pH 7.8 in a volume of ca. 3 mL. For mass spectrometry, the imidazole buffer was removed by C18 Sep-Pak (Waters, Milford, MA) cartridges. For that purpose, the peptide solution was passed through the cartridge, the silica matrix washed with water, and the peptides eluted with 100% methanol. Finally, methanol was removed by speed-vac evaporation, and the peptides were dissolved in water. In some cases, imidazole-eluted peptides were precipitated with 5% trichloracetic acid (TCA). Peptides were pelleted by centrifugation (45 000 × *g*, 30 min) and the pellet washed twice with cold 100% ethanol. Peptides were resolved in 50 μL water or 50 μL 5% acetic acid.

In some experiments, the chromopeptide was directly cleaved with trypsin on the Ni^{2+}- NTA agarose matrix. For that purpose, the peptides from a V8 holoprotein digest were passed through the column as above, the column was first washed with 20 mL Tris buffer and then with 20 mL water. Thereafter, 100 μg trypsin, dissolved in 1 mL water, was mixed with the affinity gel in the column. After 3 h

incubation at room temperature, the released peptides were collected through the column outlet in a volume of 2 mL.

The efficiency of proteolysis and chromatography was probed by PAGE. Peptides were separated on 4−12% Tris-Tricine NuPage Gels (Invitrogen, Paisley, UK) according to manufacturers instructions. Before staining the gel with coomassie, the chromopeptide was detected by Zn^{2+}-induced fluorescence (*8*, *17*).

Mass Spectrometry Characterization. Peptide samples were mass analyzed by MALDI-TOFMS and target peptides sequenced by nESI-IT MS/MS (*18*, *19*). The MALDI-TOFMS analysis was performed using a Voyager DE-PRO (Applied Biosystems, Barcelona, Spain) instrument in the reflectron mode. Spectra were externally mass calibrated using a standard peptide mixture. For the analysis, 0.5 μL of the peptide extract and 0.5 μL of matrix (∝-cyano-4-hydroxycinnamic acid, 5 mg/mL or dihydroxy benzoic acid, 10 mg/mL) were loaded in the MALDI plate.

Selected peptides were sequenced on a Finnigan LCQ ion trap mass spectrometer (ThermoQuest, Finnigan MAT, San Jose, CA) equipped with a nanospray source (Protana, Odense, Denmark). The spray voltage applied was 0.85 kV and the capillary temperature was 110 °C. For MS/MS and MS^3 experiments, the isolation window was 3 and 4 mass units wide, respectively, and the relative collision energy was selected between 30% and 40% depending of the charge of the precursor ion. Samples were desalted prior the analysis with C18 ZipTip pipet tips (Millipore, MA) following standard procedures.

Enzymatic digestion of the affinity purified sample was performed with trypsin (Promega, Madison, WI) following conventional procedures. In short, 10 μL of affinity purified sample was evaporated to dryness and redissolved in 15 μL of 50 mM ammonium bicarbonate containing 100 ng of trypsin. The incubation was carried out at 37 °C for 3 h.

Computer Alignment. Database searches were performed via NCBI BLASTP (http://ncbi.nlm.nih.gov) using Agp1 and Cph1 (*8*) as template. Many but not all of the identified phytochrome-homologous proteins have already been mentioned in earlier publications (*1*, *11*). The *Aspergillus fumigatus* phytochrome sequence was translated from assembled shotgun sequences from the site of the genome project (http://www.tigr.org/tdb/e2k1/afu1/). All protein sequences were submitted to the PFAM Internet software tool (http://www.sanger.ac.uk) for identification of protein domains. Only sequences with a GAF and a PHY domain were selected as phytochrome homologues. Protein alignments were performed with ClustalX version 1.8 (*20*). The "gap opening" and "gap extension" parameters were set to 40 and 0.4, respectively, otherwise default parameters were used. The *Neurospora crassa* Phy1 sequence required further manual adjustments in the region around the putative chromophore attachment site, because the sequence contains several obvious insertions that remained unrecognized by ClustalX.

RESULTS

Initial Proteolysis and Chromopeptide Purification. On the basis of site-directed mutagenesis experiments, it is proposed that BV is covalently bound to Cys^{20} of Agp1 (*11*). During initial trials to characterize the BV attachment site by mass spectrometry, we digested apo- and holoprotein with trypsin and subjected the fragments to MALDI-TOFMS. By comparing spectra of both samples, it might be possible to detect a fragment that can be attributed to the chromopeptide. However, on the background of a large number of proteolytic fragments, it was not possible to identify the chromopeptide (data not shown). Therefore, we decided to purify the chromopeptide after proteolysis. For that purpose, the Agp1 expression construct was re-engineered to allow affinity purification of the expected fragment. The new construct, pAG1-M13, encodes for a protein, Agp1-M13, which has an N-terminal poly-histidine-tag (his-tag) and which lacks amino acids $2-10^1$ of wild-type Agp1. In the new protein, one trypsin cleavage site N-terminal of Cys^{20} is retained, but both Endoproteinase Glu-C (V8) sites N-terminal of Cys^{20} are lost (see Figure 2). Thus, V8 digestion of holo-Agp1-M13 should release a chromopeptide which can be purified via the N-terminal his tag.

Initially, the full length Agp1-M13 product was purified as apoprotein by affinity chromatography. The purified protein incorporated biliverdin (BV) in a covalent manner and gave a photoactive adduct, which was spectrally indistinguishable from BV-Agp1 (Figure 3). Therefore, amino acids 2−10 of Agp1 are dispensable for chromophore assembly and photoconversion. This result was not unexpected because these amino acids show no significant sequence homology with N-termini of other phytochromes.

FIGURE 2: Primary structure of the N-terminal part of Agp1 and Agp1-M13. Arrows indicate the proposed protease cleavage sites (→ for trypsin and filled arrow for V8). The cysteine which is the proposed chromophore binding site is printed white on black.

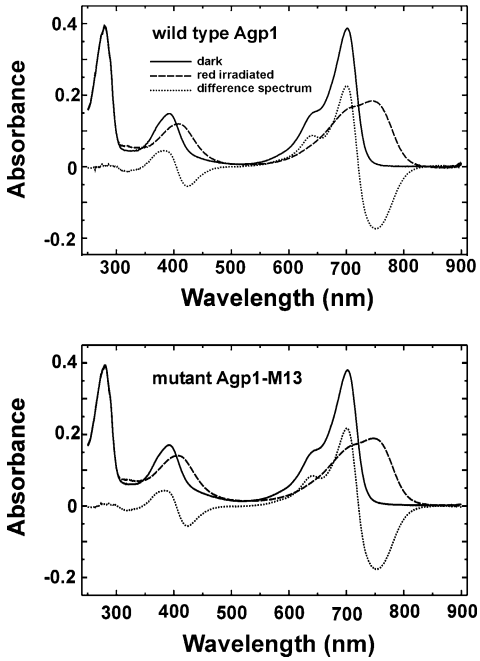

FIGURE 3: Absorbance and difference spectra of BV-adducts of wild-type Agp1 and the mutant M13.

Table 1: MALDI-TOFMS m/z Values for the Apo- and Holopeptides Detected in the V8 and V8 + Trypsin Digests of Agp1[a]

tentative peptide assignation	monoisotopic mass for M + H ion		
	calcd	exp	peak top mass (exp)
V8 Treated			
E33 apo: MHHHHHHSSHTPKLDSCGAEPIHIPGAIQE	3340.56	3340.73	3342.96
E33 holo: MHHHHHHSSHTPKLDSC**x**GAEPIHIPGAIQ E	3920.80	3921.08	3925.26
V8 + Trypsin Treated			
L17-E33 apo: LDSCGAEPIHIPGAIQE	1749.85	1749.97	1750.95
L17-E33 holo: LDSC**x**GAEPIHIPGAIQE	2330.08	2330.27	2332.29

[a] "x" stands for BV derivatization. Calculations for the *m*/*z* values of holopeptides are based on a BV mass of 580, which corresponds to an oxidized form (see text). Experimental monoisotopic masses (those corresponding to the lightest isotopic signal for each ionic species) are obtained from enlarged printouts of the spectra. For convenience, the table also includes the "peak top masses" automatically labeled in the spectra presented in figures. These values correspond to the *m*/*z* values of the more intense isotopic signal. For the compounds studied, the labeled peak top mass can be up to 3 Da higher than the experimental monoisotopic mass (compare, e.g., Figure 5).

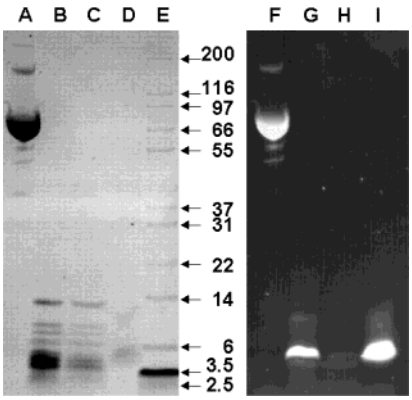

FIGURE 4: Proteolysis and affinity purification of the Agp1-M13 BV adduct. Peptides were electrophoretically separated on NuPage gels. Chromopeptide fragments were visualized by Zn^{2+}-induced fluorescence (lanes F−I). Thereafter, the same gel was stained with Coomassie (lanes A−E). Lanes: A and F, full-length Agp1-M13, BV adduct after affinity purification; B and G, the same sample after V8 proteolysis, and this sample was applied to the Ni^{2+}-affinity column; C and H, flow-through of affinity column; D and I, peptide eluted from the column by 250 mM imidazole; E, marker proteins, molecular weight in kDa indicated on the right side of the panel.

It is possible that the codon for Met^{10} of Agp1 serves as second translation start in the natural host.

Digestion of BV-Agp1-M13 by V8 protease was optimized to obtain a small chromophore-bearing peptide. To test for the size of the chromopeptide, samples were electrophoretically separated on NuPage gels and the chromophore detected by Zn^{2+}-induced fluorescence (see Experimental Procedures). The smallest chromopeptide fragment was obtained in buffer containing SDS. This fragment had an apparent molecular weight of ~5 kDa on NuPage gels (Figure 4, lane G). As outlined above, the chromopeptide should contain the his tag and thus be purified by Ni^{2+} affinity chromatography. This purification was performed after diluting the sample to reduce the concentration of SDS, which interferes with the histidine/Ni^{2+} interaction. Binding of the blue-green chromopeptide to the column matrix was directly visible, whereas the flow-through was free of chromophore-bearing peptides, as judged by Zn^{2+} fluorescence (Figure 4, lane H). Free BV does not interact with the Ni^{2+} affinity matrix. Therefore, BV was still bound to the peptide, presumably to a ~5 kDa fragment of the N-terminus of Agp1.

The chromopeptide was eluted from the column with 250 mM imidazole (Figure 4, lane I), but not with acidic buffer. HPLC UV/VIS analysis that was performed after removal of imidazole showed that the sample contained one single chromopeptide species and no free BV (data not shown). When Agp1-M13 apoprotein was processed in the same manner as the holoprotein, a single nonfluorescent band with an apparent size of ~4 kDa was stained in the NuPage gels (data not shown). For some MS measurements, we cleaved the Ni^{2+}-NTA-bound chromopeptide directly on the affinity matrix with trypsin. The trypsin treatment resulted in a release of chromophore from the gel as judged by optical spectroscopy. There is one trypsin cleavage site, Lys^{16}, between the N-terminal his-tag and the putative chromophore binding Cys^{20} (Figure 2).

Mass Spectrometry. The affinity purified holopeptide was subjected to MALDI and electrospray mass spectrometry analysis. Although V8 digestion of the holoprotein was expected to yield the corresponding Glu^{23} peptide, this ion was not observed in the MALDI-TOFMS analysis. The MALDI spectrum showed, however, two signals at *m*/*z* 3925.26 and 3342.96 that were attributed to the Glu^{33} holopeptide and Glu^{33} apopeptide, respectively (Figure 5 a and Table 1). The mass increase of 580 does not exactly match with the mass of BV, which is 582, but rather correspond to an oxidized form of BV, which is present in all preparations (see also below). The assignation of the Glu^{33} holopeptide was first confirmed by PSD analysis, which gave three major signals centered at *m*/*z* 583.7 (protonated BV ion), 1821.5 (b15 ion), and 3344.4 (loss of BV from the peptide ion, data not shown).

Two other prominent signals, centered at 583.58 and 1838.38, can be attributed to the BV chromophore and the Asp^{18} peptide, respectively (Figure 5a). The latter peptide is most likely released by V8 protease, which has a weak aspartate activity. Its identity was confirmed by MS/MS measurements (data not shown). The signal centered at 3479.97 might be attributed to the Glu^{33} chromopeptide in which the chromophore was cleaved between the ring A and ring B. The size difference of 137 between this fragment and the apopeptide corresponds to the mass of the ring A of BV with one methyl group ($C_8H_{11}NO$).

When the apoprotein was treated with V8 protease and processed in the same way as the holoprotein, MALDI measurements revealed a signal at *m*/*z* 1838.92 (Figure 5 b), which corresponds to the Asp^{18} peptide. Thus, the apoprotein is completely cleaved by the protease between Asp^{18} and Ser^{19}. The different cleavage V8 pattern between

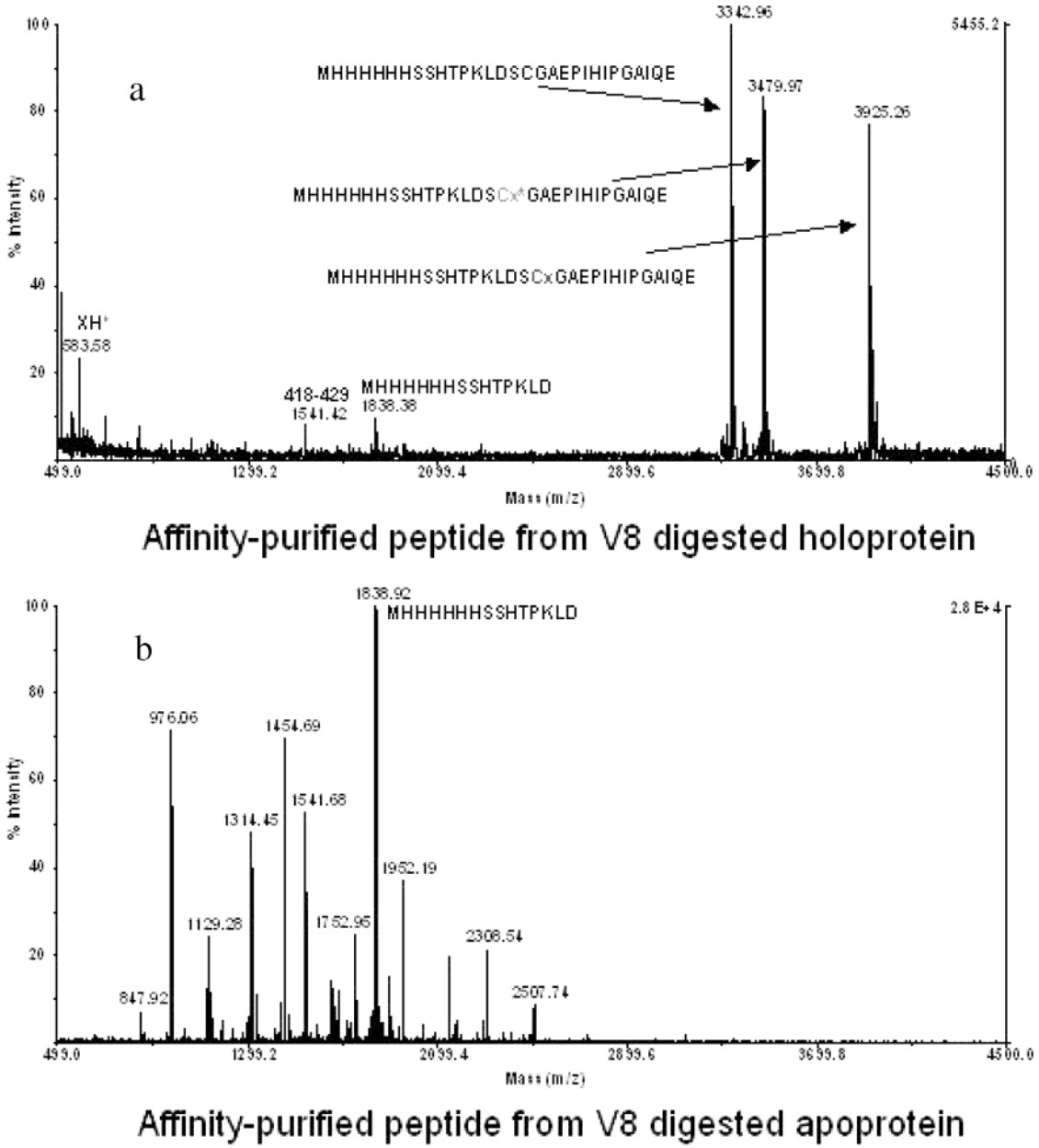

FIGURE 5: MALDI TOFMS analysis of the affinity purified peptide extract from the V8 digestion of BV-assembled Agp1-M13 (a) and Agp1-M13 apoprotein (b). After affinity chromatography, imidazole was removed using C-18 cartridges.

apo- and holoprotein implies that the chromophore can mask the Asp^{18} cleavage site.

To locate the BV molecule in the chromopeptide sequence, the affinity-purified peptide extract was submitted to nESI-ITMS after purification using a C_{18}-ZipTip. However, we could not detect any signal from the holopeptide in the extract. As the holopeptide was clearly detected when the ZipTip eluate was reanalyzed by MALDI-TOFMS, we attributed the former negative results to a deleterious effect of the holopeptide his-tag chain on nESI ionization. To render the peptide amenable for nESI sequenciation, we eliminated the his tag by treating the affinity-purified extract of the V8 digest with trypsin (see Figure 2 for cleavage site). The resulting digest was purified using a C_{18} ZipTip and reanalyzed by nESI-ITMS. The doubly charged ion of the Agp1[17−33] holopeptide (LDSCxGAEPIHIPGAIQE, *m*/*z* 1166.4) was isolated in the trap and fragmented at 30% collision energy. The product ion spectrum showed y and b series of fragment ions that confirmed the sequence of the peptide and the presence of BV (Figure 6). In addition to the holopeptide derived fragment ions, several ions corresponding to a cystine-bound dimer of the apopeptide were observed (labeled with ∗ in Figure 6). This identification was confirmed by MS^3 analysis (data not shown). The occurrence of this dimer could be an artifact formed during sample preparation, and its presence in the MS/MS spectrum is due to the practically coincident *m*/*z* values of the triply charged ion of the dimer and the doubly charged ion of the Agp1[17−33] holopeptide.

The presence of the BV molecule in the structure was confirmed by a fragment ion at *m*/*z* 581.3 that corresponds to oxidized BV ($[BV-H]^+$). This ion was also observed in the PSD analysis of the holopeptide together with the BV + H ion at *m*/*z* 583 (ratio 583/581 = 1.7) and is indicative of the facility with which the polyunsaturated structure of BV can undergo redox processes. It is not clear whether this ratio

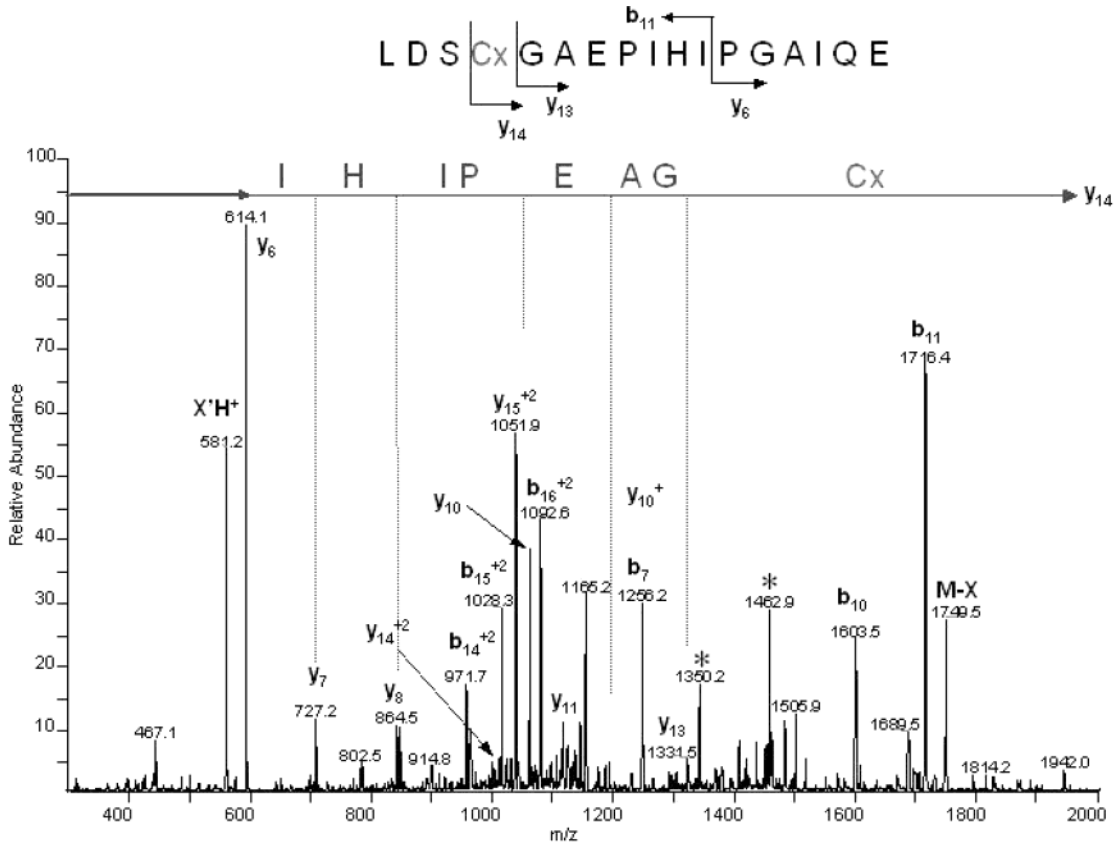

FIGURE 6: Nanospray MS/MS sequence spectrum obtained by fragmentation of the doubly charged ion of the Agp1[17−33] holopeptide. The affinity-purified chromopeptide was precipitated with TCA, resuspended in water and cleaved with trypsin. Signals indicated with an asterisk correspond to fragment ions from the Cys-bound dimer of the holopeptide (see text). $X'H^+$ oxidized BV ion.

reflects the actual BV composition in the apopeptide or whether BV oxidation is also affected by the ionization method. The presence of the oxidized/reduced forms of BV affects also the relative abundance of the corresponding holopeptide molecules. Most of the spectra presented here were obtained from holopeptide extracts with isotopic distributions of the protonated peptide ions indicating the presence of mainly the oxidized form of BV (a mass difference of 580 between apo and holopeptide, see above also). Several sample handling procedures including evaporation and storage were shown to increase the abundance of the reduced form in these extracts.

Peptide-bound BV was located at Cys^{20} of modified Agp1 on the basis of the *m*/*z* values of the single charged y_{13} and doubly charged y_{14} ion fragments (Figure 6). A zoom scan of the doubly charged y_{14} is shown in the inset of Figure 7 a. The identity of this ion was confirmed by MS^3 analysis (Figure 7a). This spectrum revealed the release of the chromophore (signals at *m*/*z* 581 and 583) and the y_6 ion, which is also seen in the MS/MS spectrum (compare Figure 6). The MS^3 fragmentation of the b_{11} fragment ion (LDSCx-GAEPIHI, *m*/*z* 1719) showed an LDS peptide tag (Figure 7 b) where serine was unmodified in agreement with the observation that BV is in the Cys^{20} position.

The trypsin-digested sample contained also an nESI-ITMS signal of the doubly charged Agp1[17−33] peptide which could carry the ring A ring of BV (LDSCx*GAEPIHIP-GAIQE) at *m*/*z* 944. When this ion was fragmented, the MS/MS spectrum revealed almost the entire peptide sequence and showed that the cysteine is modified by a 137 Da residue (Figure 8), which might result from a reduced ring A pyrrol ring of the chromophore ($C_8H_{11}NO$).

Distribution of the Covalent Binding Site. In an earlier paper, we noted that several other bacterial phytochromes have a cysteine residue at a position homologous to Cys^{20} of *Agrobacterium* Agp1 (*11*). To obtain an overview about sequences known to date, we searched again public databases for phytochrome-like proteins. We restricted our search to proteins with an N-terminal chromophore module containing a GAF and a PHY domain. Some less related cyanobacterial proteins have been denominated phytochrome-like proteins based on their sequence homology with the GAF domain of phytochromes (*21*−*24*). These phytochrome-like proteins were not included in our analyses. We performed a ClustalX alignment with the N-terminal chromophore module (see Figure 1) of 29 putative bacterial phytochrome protein sequences, three sequences from fungi and representative plant sequences. This alignment showed that all known (putative) typical phytochromes follow a general rule: either they have a cysteine homologous to Cys^{20} of Agp1, or they have a cysteine within the GAF domain, homologous to the chromophore-binding cysteine of plant phytochromes (Table 2). The first group comprises all bacterial proteins with the exception of some cyanobacterial species. Fungal phytochrome homologues also belong to this group. Quite interestingly, one protein from the plant pathogen *Pseudomonas syringae*, termed BphP2 here, has cysteines at both positions. It is obvious that all known (putative) typical phytochromes

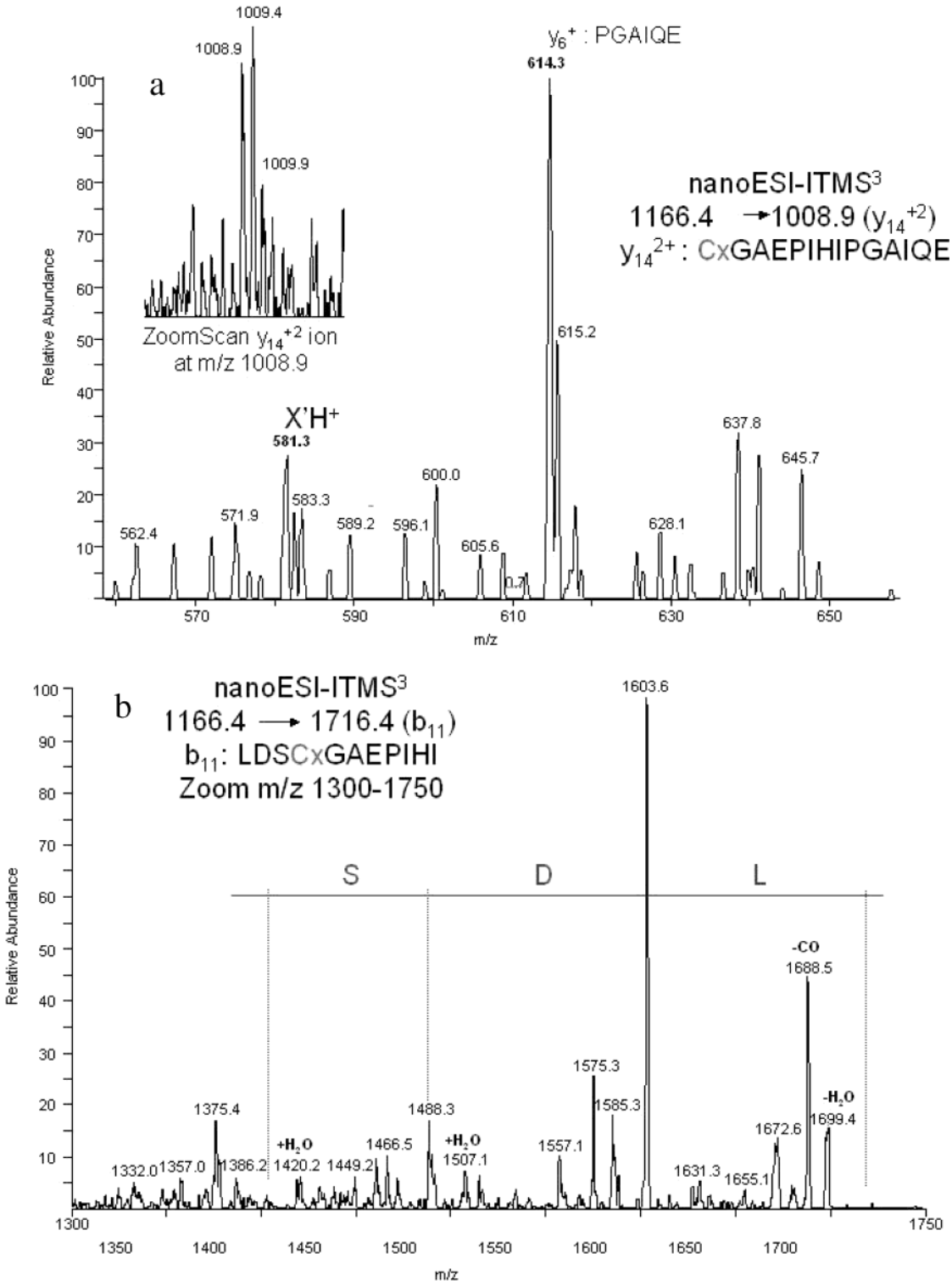

FIGURE 7: (a) Nanospray MS^3 spectrum obtained with the y_{14}^{2+} ion confirming the identity of the selected ion. Sample preparation was performed as in Figure 6. Note the signals of BV and oxidized BV at *m/z* 583 and 581, respectively. Inset: zoom scan of the selected y_{14}^{2+} ion in nanospray MS/MS. The 0.5 *m/z* difference between the isotopes shows that the ion has a double charge. (b) Nanospray MS^3 spectrum of the b_{11} product ion from the holopeptide doubly charged ion showing an unmodified LDS peptide tag.

bind the chromophore in a covalent manner, although noncovalent association can also give photoactive adducts with light-regulated histidine-kinase activity (*11*, *13*, *25*).

Role of Histidine 250. On the basis of mutant analyses and mass spectrometry, it has been proposed that *Deinococcus* phytochrome DrBphP attaches the chromophore via a histidine residue which is highly conserved in phytochromes and lies immediately C-terminal next to the chromophore binding cysteine of plant phytochromes (*10*). To test for the role of the homologous histidine 250 in Agp1, we mutated this amino acid to alanine (H250A) and tested for chromophore-protein interaction, covalent attachment and spectral properties. After mixing chromophore and protein, an adduct was obtained which is spectrally comparable with the Pr form

Table 2: Amino Acid Sequence of Phytochrome Homologues in the Region of the Two Possible Chromophore Binding Cysteines[a]

species name, phytochrome	group	accession number	region around chromophore binding C20 of Agp1	region around chromophore-binding cysteine of plant phytochrome
Arabidopsis thaliana, PhyA	Plants	NP_172428	RSDKVTTLYLHHIQK	TLRAPHSCHLQYMAN
Synechocystis PCC6803, Cph1	Cyanobacteria	Q55168	SDQSLRQLETLAIHT	ILRSAYHCHLTYLKN
Nostoc PCC7120, CphA	Cyanobacteria	Q9LCC2	QNINVTSLKEAPIHL	ILRSAANCHLEYLHN
Nostoc PCC7120, CphB	Cyanobacteria	NP_486939	FQVDLSNCSKEPIHI	VLRSVSPLHIEYMQN
Tolopothrix PCC7601, CphA	Cyanobacteria	AAL76159	QSINVNSLKEAAIHV	ILRTAANCHLEYLHN
Tolopothrix PCC7610, CphB	Cyanobacteria	AAL76161	FEVDLTNCDREPIHI	VLRSVSPLHIEYLHN
Nostoc punctiforme, CphA1	Cyanobacteria	ZP_00109399	QAEALTNLDRKPIHI	LLRSFDWCCAEYHQN
Nostoc punctiforme, CphA2	Cyanobacteria	ZP_00107118	PGINLISLKEAPIHI	ILRSAASCHTEYLHN
Agrobacterium tumefaciens, Agp1	α proteobacteria	NP_354963	HTPKLDSCGAEPIHI	QLRSVSPVHLEYMRN
Agrobacterium tumefaciens, Agp2	α proteobacteria	NP_355125	YHVDLTNCDREPIHI	HLRSVSPLHCEYLRN
Rhodopseudomonas palustris, BphP1	α proteobacteria	ZP_00011118	GTADLSNCEREEIHL	FLRSMSPLHLQYLKN
Rhodopseudomonas palustris, BphP2	α proteobacteria	NZ_AAAF01000001	RQPDLSTCDDEPIHI	ILRSVSPVHLEYMRN
Rhodospirillum centenum, Ppr	α proteobacteria	AAD22391	EVVDFSVCEQEDIRR	RHRSLSPVHLQYLRN
Rhodobacter sphaeroides, BphP	α proteobacteria	AAL50635	GTFDPSICEMEPIAT	SLRSVSPVHLDYMQN
Rhizobium legominosarum, BphP	α proteobacteria	CAC95194	EPVDLTNCDREPIHQ	VLRSVSPLHIEYLKN
Bradyrhizobium spec., BphP	α proteobacteria	AL68700	GHATLANCEREQIHL	CLRSMSPLHQKYLQN
Pseudomonas aeruginosa, BphP	χ proteobacteria	NP_252806	TPVTLANCEDEPIHV	VLRSVSPLHCEYLTN
Pseudomonas putida, BphP1	χ proteobacteria	NP_744505	LADAMERCAQEPIQV	ALRSVSPVHLQYMRN
Pseudomonas putida, BphP2	χ proteobacteria	AAL50633	PQVNLTNCDREPIQI	HLRSVSPLHCEYLCN
Pseudomonas fluorescens, BphP	χ proteobacteria	AAL50631	FEELLANCADEPIRF	TLRSVSPLHCQYMKN
Pseudomonas syringae, BphP1	χ proteobacteria	NP_791725	FEVLLANCADEPIQF	TLRSVSPLHCQYMKN
Pseudomonas syringae, BphP2	χ proteobacteria	ZP_00126919	LEAALAECAREPIRV	RSVSPVHCEYLKNMG
P. syringae var tomato, BphP2	χ proteobacteria	NP_7924609	LEAALAECAREPIRI	TLRSVSPVHCEYLKN
Xanthomonas axonopodis, BphP	χ proteobacteria	AE012082	EPLDMDVCAQEPIHI	SLRSVSPVHLEYLAN
Xanthomonas campestris, BphP	χ proteobacteria	NP_639488	NPLDLDVCAREPIHI	SLRSVSPVHLEYLAN
Deinococcus radiodurans, BphP	Deinococci	NP_285374	PEITTENCEREPIHI	VLRATSPVHMQYLRN
Cytophaga hutchinsonii, BphP1	Sphingobacteria	ZP00117110	DLVNLQNCDQEPIHI	VLRSVSPLHVQYLHN
Cytophaga hutchinsonii, BphP2	Sphingobacteria	ZP00117156	QNYDSKFCGSLPIHI	NLRGVIKVHLEYLTN
Neurospora crassa, Phy1	Fungi	EAA31157	RDGQLQRCEDEPIRF	YLRAMSPLHLKYLAN
Neurospora crassa, Phy2	Fungi	EAA30814	ARRAFTTCDEEPIHI	YLRAMSPVHLKYLSN
Aspergillus fumigatus, Phy	Fungi		ANDSYQACEDEPIHI	YLRAMSPLHLKYLAN

[a] Homologous cysteines are printed white on black; if another amino acid is located at the homologous position, it is printed white on gray. For plant phytochromes, *Arabidopsis* PhyA is shown as the only representative. The other 50 plant sequences analyzed had the same cysteine pattern. The conserved histidine which is the proposed attachment site for *Deinococcus* phytochrome is printed black on gray (further details see text).

of the wild-type adduct (see Figure 9). Upon irradiation with red light, the absorbance decreased and shifted to lower wavelengths. This spectrum differs drastically from that of the wild-type adduct (compare Figure 3) but resembles the spectrum of the free chromophore. We then tested for the strength of chromophore−protein interaction with BV and PCB in the native state (Table 3). The latter chromophore is associated in a noncovalent manner to the Agp1 protein, because its ring A side chain differs from BV (*13*). The assay was performed either with unmodified protein or with protein in which cysteine residues were blocked by 1 mM 5,5′-dithiobis(2-nitrobenzoic acid) (DTBN). This treatment inhibits covalent BV attachment (*11*). Thus, in three of the four different assays shown in Table 3, the chromophore can bind to the protein only in a noncovalent manner. The percentage of chromophore bound to the wild type protein was high in all four cases. For this protein, a tight interaction does obviously not rely on covalent ligation. In the case of the mutant, a strong binding was only observed when the nonblocked protein was mixed with BV. In all other cases, chromophore binding to H250A was weak (Table 3). Thus, a tight chromophore-protein interaction in the H250A mutant seems only possible if a covalent link can be formed. After the column purification of the native BV-H250A adduct in the native state, the sample was mixed with SDS to dissociate noncovalent interactions. During a second column separation, all chromophore appeared to migrate together with the protein (Figure 9, lower panel). This test showed that BV is indeed covalently bound to Agp1-H250A.

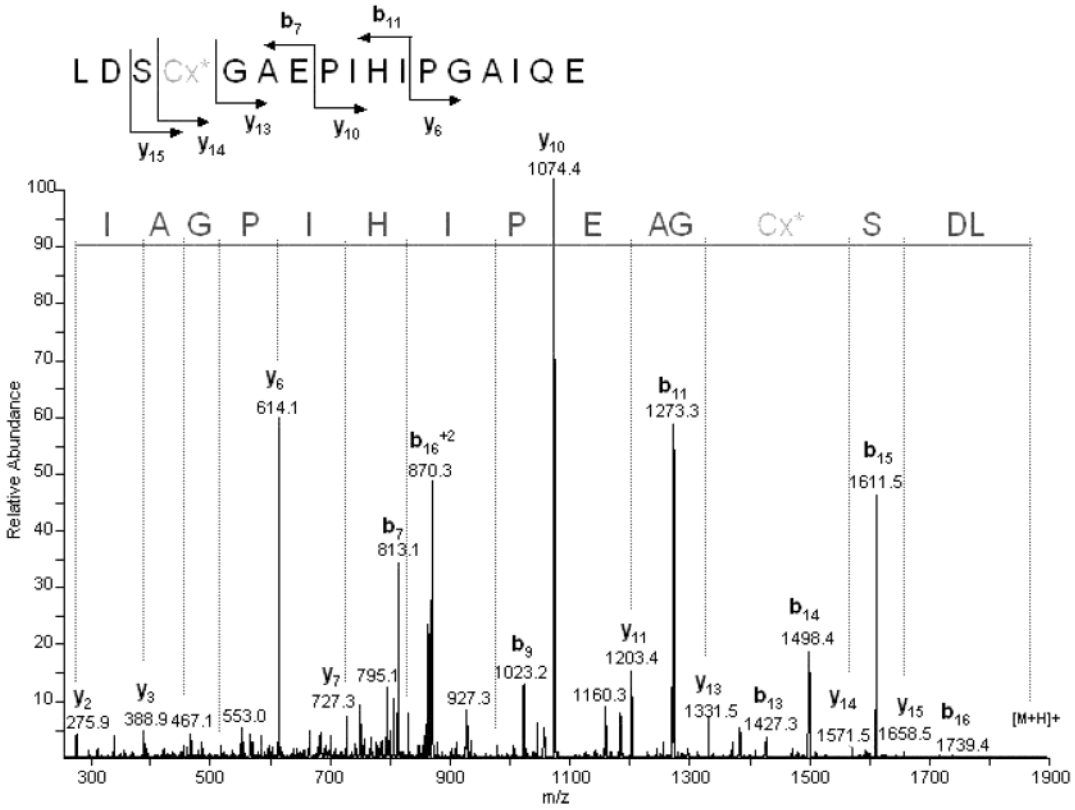

FIGURE 8: Nanospray MS/MS sequence spectrum obtained by fragmentation of the doubly charged ion of the modified Agp1[17−33] peptide (*m/z* 944). The holopeptide was directly released from the affinity matrix by trypsin digestion. x* is presumably cleaved BV. Note that the 240 da size difference between y_{13} and y_{14} corresponds to the mass of cysteine (103) which is modified by a 137 da side group (see text).

DISCUSSION

On the basis of site-directed mutagenesis, it has been proposed that Cys^{20} is the covalent attachment site for the BV chromophore of *Agrobacterium* phytochrome Agp1. However, an indirect role of Cys^{20} could not be excluded. For example, this amino acid might be essential for the enzymatic lyase activity. Although this possibility is unlikely, we found it important to identify the chromophore binding site by an independent method. With the present approach it could be shown in the first step that the chromophore attachment site is indeed located within the N-terminal ~5 kDa of the protein. This was possible by a combination of protein re-engineering, V8-proteolysis, and affinity purification, during which the chromophore was eluted together with the N-terminal affinity tag (Figure 4). In the next step, MALDI-TOFMS mass determination of the purified chromopeptide gave information on the cleavage site that had generated the peptide, and confirmed the mass of the holopeptide (Figure 5a). It turned out that the V8 protease cleaves behind Glu^{33}, but not behind Glu^{23}. It is known that proline inhibits the action of trypsin, when located next to lysin or arginine. Pro^{24} could similarly mask the V8 cleavage site at Glu^{23}. The MALDI-TOFMS spectra of the purified fragment contained signals of the holopeptide, the apopeptide and the free chromophore, which implies that the chromophore is partially cleaved from the peptide during MS sample preparation or laser ionization. The possibility that the chromophore is lost during earlier steps is excluded, since the holopeptide band was clearly visible on NuPage-gels by Zn^{2+}-fluorescence. There was no indication for an apopeptide band which would have been detected by its higher mobility. Another prominent signal in the MALDI-TOFMS is most likely related to the peptide with a remaining "broken" chromophore. The mass of this ion is 137 units larger than that of the apopeptide. The calculated mass of the modified pyrrole ring A (C_8H_9NO), which results from a cleavage between rings A and B of BV, is 135. The mass of 137 Da belongs most likely to a reduced form of this ring ($C_8H_{11}NO$).

To locate the exact position of the binding site within the chromopeptide, nanoelectrospray tandem mass spectrometry was performed with the trypsin-digested fragment. The y_{13} and y_{14} signals in the MS/MS spectra differ by the mass of cysteine with an attached BV residue (Figure 6). These analyses confirmed the role of Cys^{20} as covalent attachment site for BV. Also, MS^3 analyses with selected fragments confirmed the role of the cysteine (Figure 7). The MS/MS spectra of the peptide with the "broken" chromophore showed that the 137 Da residue is bound to that amino acid (Figure 8).

Taken together, the results of proteolysis and mass spectrometry clearly show that BV is covalently attached to the cysteine 20 residue of Agp1. As shown in an earlier paper (*13*), the ring A vinyl side chain of BV is required for covalent attachment. We propose that this group forms a thioether link with the sulfur of the cysteine residue. Thioether formation between vinyl side chains and cysteine residues of the protein is known for, e.g., the heme cofactor in cytochrome *c* (*26*).

The cysteine residue is highly conserved among phytochromes. With the exception of plant phytochromes and the above-mentioned subgroup of cyanobacterial orthologs, all

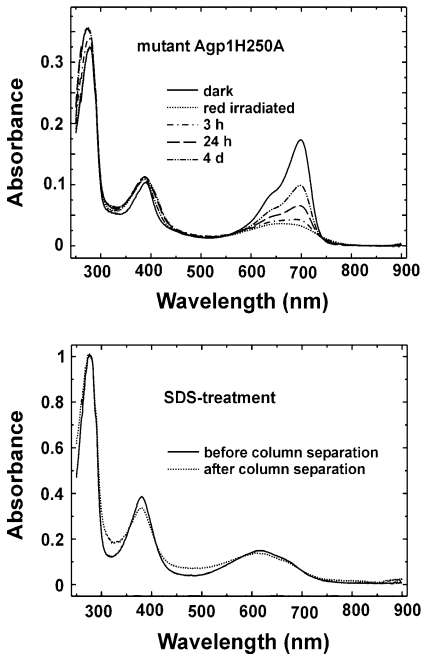

FIGURE 9: Absorbance spectra of the Agp1 H250A mutant after BV assembly. About 10 μM protein were mixed with 6 μM BV. Before the assays, free chromophore was removed using desalting columns. The panel above shows the spectrum before irradiation (Pr form), after red irradiation and the slow recovery of the Pr form during a prolonged dark incubation of up to 4 d. The panel below shows spectra after SDS denaturation of the same holoprotein, before and after column separation. These spectra are normalized to the protein absorbance maximum at 280 nm. From comparing both spectra in the range of chromophore absorbance (350−700 nm), it can be judged that the chromophore coelutes with the protein and is thus covalently bound.

Table 3: Amount of Chromophore Bound to Agp1 Wild Type and the H250A Mutant in the Native State after Column Separation[a]

			Cys blocked by DTBN	
	BV	PCB	BV	PCB
wild-type Agp1	(99 ± 1)%	(93 ± 2) %	(84 ± 1) %	(95 ± 3) %
H250A	(75 ± 2) %	(23 ± 3) %	(16 ± 3) %	(29 ± 4) %

[a] Apoprotein (10 μM) was mixed with BV or PCB (4 μM) and passed through a desalting column. In some cases, the protein was preincubated with DTBN, which inhibits covalent chromophore attachment. The values were estimated by comparing UV/VIS spectra after and before column separation. Mean values of four replicate experiments ± SE.

typical phytochrome-homologues contain that cysteine residue. The homology has already been noted for some bacterial phytochromes with documented chromophore assembly and photoactivity (*11*). Here we found that also three fungal phytochrome-homologous proteins and Ppr from *Rhodospirillum centenum* contain that cysteine. The latter protein has a phytochrome-like domain arrangement, but is N-terminally extended by a photoactive-yellow-protein domain (*27*). In our database search, other yet unpublished prokaryotic phytochrome-homologues appeared, all with a cysteine at the homologous position. These include proteins from the plant pathogens *Pseudomonas syringae*, *P. fluorescens*, *Xanthomonas campestris*, and *X. axonopidos*.

The position of the chromophore attachment site was quite surprising: The highest degree of homology among phytochromes is in the region of the GAF-domain. This region contains the chromophore attachment site of plant phytochromes and other amino acids important for protein−chromophore interaction (*28*−*30*). A weaker related phytochrome homolog, Cph2 from the cyanobacterium *Synechocystis*, has two GAF domains, but shows no homology with the N-terminus of Agp1 or other conventional phytochromes (*23*, *31*). Because Cph2 assembles to a photoactive adduct, it could be suggested that the N-terminal part of conventional phytochromes is dispensable for assembly and photoactivity. However, mutant studies preformed with recombinant plant phytochrome show that the N-terminal region plays a critical role for chromophore ligation (*28*). Secondary structure predictions identify a PAS domain in the N-terminal part of several prokaryotic phytochromes. This PAS-like domain (PLD) is located next to the chromophore-binding cysteine (see Figure 1) and could function as chromophore interaction site (*13*). The specific function of the various regions of phytochromes is as yet only poorly understood and requires further analyses, but the data taken together suggest that both the N-terminal PLD and the GAF domain are important for lyase, chromophore interaction, and photoconversion, probably in all conventional phytochromes. On the basis of mutant analyses and PCB incorporation, it has been proposed that both regions are in close contact with each other (*13*).

The role of the conserved His^{250} residue was further highlighted by our studies. It is shown by studies on the H250A mutant that His^{250} is not required for covalent chromophore ligation in Agp1. However, when covalent ligation was inhibited by DTBN, the interaction between chromophore and the mutant protein was only weak. The same result was obtained with PCB, which does not form a covalent link with Agp1 (Table 3). Therefore, His^{250} seems to be required for noncovalent interaction between chromophore and protein. The function of His^{250} could be to bind and coordinate one of the rings of the chromophore, probably by π stacking. Because the spectrum obtained after photoconversion of the BV-H250A adduct resembles that of the free chromophore, we propose that light-induced chromophore isomerization reduces the interaction between protein and BV.

The fact that this histidine is highly conserved in all phytochromes points to a common function. An interaction between the homologous histidine and the ring A of the chromophore has been proposed for plant phytochromes (*28*). Since the first step in the assembly reaction is chromophore-protein binding, before the lyase can form a covalent link (*32*), it is understandable that some histidine mutants are unable to form adducts or assemble slower than wild-type proteins (*28*−*30*). The mutant results of *Deinococcus* phytochrome (*10*) are also in agreement with that theory.

ACKNOWLEDGMENT

We thank Berta Esteban for helpful discussions.

REFERENCES

1. Bhoo, S. H., Davis, S. J., Walker, J., Karniol, B., and Vierstra, R. D. (2001) Bacteriophytochromes are photochromic histidine kinases using a biliverdin chromophore, *Nature 414*, 776−779.
2. Lamparter, T. and Hughes, J. (in press) Phytochromes and phytochrome-like proteins in cyanobacteria, in *Photoreceptors and Light Signalling* (Batschauer, A., Ed.) RSC, Cambridge, U.K.
3. Starostzik, C., and Marwan, W. (1995) A photoreceptor with characteristics of phytochrome triggers sporulation in the true slime mould Physarum polycephalum, *FEBS Lett. 370*, 146−148.

4. Rüdiger, W., and Thümmler, F. (1994) The phytochrome chromophore, in *Photomorphogenesis in Plants* (Kendrick, R. E., and Kronenberg, G. H. M., Eds.) 2nd ed., pp 51−69, Kluwer Academic Publishers, Dordrecht, The Netherlands.
5. Kidd, D. G., and Lagarias, J. C. (1990) Phytochrome from the green alga *Mesotaenium* caldariorum. Purification and preliminary characterization, *J. Biol. Chem. 12*, 7029−7035.
6. Hübschmann, T., Börner, T., Hartmann, E., and Lamparter, T. (2001) Characterisation of the Cph1 holo-phytochrome from *Synechocystis* sp. PCC 6803, *Eur. J. Biochem. 268*, 2055−2063.
7. Wahleithner, J. A., Li, L. M., and Lagarias, J. C. (1991) Expression and assembly of spectrally active recombinant holophytochrome, *Proc. Natl. Acad. Sci. U.S.A. 88*, 10387−10391.
8. Lamparter, T., Mittmann, F., Gärtner, W., Börner, T., Hartmann, E., and Hughes, J. (1997) Characterization of recombinant phytochrome from the cyanobacterium Synechocystis, *Proc. Natl. Acad. Sci. U.S.A. 94*, 11792−11797.
9. Jorissen, H. J., Quest, B., Remberg, A., Coursin, T., Braslavsky, S. E., Schaffner, K., Tandeau de Marsac, N., and Gärtner, W. (2002) Two independent, light-sensing two-component systems in a filamentous cyanobacterium, *Eur. J. Biochem. 269*, 2662−2671.
10. Davis, S. J., Vener, A. V., and Vierstra, R. D. (1999) Bacteriophytochromes: Phytochrome-like photoreceptors from nonphotosynthetic eubacteria, *Science 286*, 2517−2520.
11. Lamparter, T., Michael, N., Mittmann, F., and Esteban, B. (2002) Phytochrome from *Agrobacterium tumefaciens* has unusual spectral properties and reveals an N-terminal chromophore attachment site, *Proc. Natl. Acad. Sci. U.S.A. 99*, 11628−11633.
12. Giraud, E., Fardoux, J., Fourrier, N., Hannibal, L., Genty, B., Bouyer, P., Dreyfus, B., and Vermeglio, A. (2002) Bacteriophytochrome controls photosystem synthesis in anoxygenic bacteria, *Nature 417*, 202−205.
13. Lamparter, T., Michael, N., Caspani, O., Miyata, T., Shirai, K., and Inomata, K. (2003) Biliverdin binds covalently to *Agrobacterium* phytochrome Agp1 via its ring A vinyl side chain, *J. Biol. Chem. 278*, 33786−33792.
14. Aravind, L., and Ponting, C. P. (1997) The GAF domain: an evolutionary link between diverse phototransducing proteins, *Trends. Biochem. Sci. 22*, 458−459.
15. Hughes, J., Lamparter, T., Mittmann, F., Hartmann, E., Gärtner, W., Wilde, A., and Börner, T. (1997) A prokaryotic phytochrome, *Nature 386*, 663.
16. Lamparter, T., Esteban, B., and Hughes, J. (2001) Phytochrome Cph1 from the cyanobacterium *Synechocystis* PCC6803: purification, assembly, and quaternary structure, *Eur. J. Biochem. 268*, 4720−4730.
17. Berkelman, T. R., and Lagarias, J. C. (1986) Visualization of bilin-linked peptides and proteins in polyacrylamide gels, *Anal. Biochem. 156*, 194−201.
18. Griffiths, W. J. (2000) Nanospray mass spectrometry in protein and peptide chemistry, *EXS 88*, 69−79.
19. Roepstorff, P. (2000) MALDI-TOF mass spectrometry in protein chemistry, *EXS 88*, 81−97.
20. Thompson, J. D., Gibson, T. J., Plewniak, F., Jeanmougin, F., and Higgins, D. G. (1997) The ClustalX windows interface: flexible strategies for multiple sequence alignment aided by quality analysis tools, *Nucleic Acids Res. 24*, 4876−4882.
21. Wilde, A., Churin, Y., Schubert, H., and Börner, T. (1997) Disruption of a Synechocystis sp. PCC 6803 gene with partial similarity to phytochrome genes alters growth under changing light qualities, *FEBS Lett. 406*, 89−92.
22. Kehoe, D. M., and Grossman, R. (1996) Similarity of a chromatic adaptation sensor to phytochrome and ethylene receptors, *Science 273*, 1409−1412.
23. Wu, S. H., and Lagarias, J. C. (2000) Defining the bilin lyase domain: lessons from the extended phytochrome superfamily, *Biochemistry 39*, 13487−13495.
24. Schmitz, O., Katayama, M., Williams, S. B., Kondo, T., and Golden, S. S. (2000) CikA, a bacteriophytochrome that resets the cyanobacterial circadian clock, *Science 289*, 765−768.
25. Jorissen, H. J., Quest, B., Lindner, I., Tandeau de Marsac, N., and Gärtner, W. (2002) Phytochromes with noncovalently bound chromophores: the ability of apophytochromes to direct tetrapyrrole photoisomerization, *Photochem. Photobiol. 75*, 554−559.
26. Allen, J. W., Tomlinson, E. J., Hong, L., and Ferguson, S. J. (2002) The Escherichia coli cytochrome c maturation (Ccm) system does not detectably attach heme to single cysteine variants of an apocytochrome c, *J. Biol. Chem. 277*, 33559−33563.
27. Jiang, Z. Y., Swem, L. R., Rushing, B. G., Devanathan, S., Tollin, G., and Bauer, C. E. (1999) Bacterial photoreceptor with similarity to photoactive yellow protein and plant phytochromes, *Science 285*, 406−409.
28. Bhoo, S. H., Hirano, T., Jeong, H. Y., Lee, J. G., Furuya, M., and Song, P.-S. (1997) Phytochrome photochromism probed by site-directed mutations and chromophore esterification, *J. Am. Chem. Soc. 119*, 11717−11718.
29. Remberg, A., Schmidt, P., Braslavsky, S. E., Gärtner, W., and Schaffner, K. (1999) Differential effects of mutations in the chromophore pocket of recombinant phytochrome on chromoprotein assembly and Pr-to-Pfr photoconversion, *Eur. J. Biochem. 266*, 201−208.
30. Deforce, L., Furuya, M., and Song, P. S. (1993) Mutational analysis of the pea phytochrome A chromophore pocket: chromophore assembly with apophytochrome A and photoreversibility, *Biochemistry 32*, 14165−14172.
31. Park, C. M., Kim, J. I., Yang, S. S., Kang, J. G., Kang, J. H., Shim, J. Y., Chung, Y. H., Park, Y. M., and Song, P. S. (2000) A second photochromic bacteriophytochrome from Synechocystis sp. PCC 6803: spectral analysis and down-regulation by light, *Biochemistry 39*, 10840−10847.
32. Li, L., Murphy, J. T., and Lagarias, J. C. (1995) Continuous fluorescence assay of phytochrome assembly in vitro, *Biochemistry 34*, 7923−7930.

BI035693L